

## Article

# Hydrochemical Characteristics and Cause Analysis of Natural Water in the Southeast of Qinghai-Tibet Plateau

Zongjun Gao <sup>1</sup>, Hui Tong <sup>1</sup>, Qiao Su <sup>2,\*</sup> , Jiutan Liu <sup>3</sup>, Fasheng Gao <sup>1</sup> and Cong Han <sup>1</sup>

<sup>1</sup> College of Earth Science and Engineering, Shandong University of Science and Technology, Qingdao 266590, China; zongjungao1964@163.com (Z.G.); thsdust@126.com (H.T.); gfs@126.com (F.G.); hcsdust@126.com (C.H.)

<sup>2</sup> Key Laboratory of Marine Sedimentology and Environmental Geology, First Institute of Oceanography, Ministry of Natural Resources, Qingdao 266061, China

<sup>3</sup> College of Energy and Mining Engineering, Shandong University of Science and Technology, Qingdao 266590, China; ljtsdust@126.com

\* Correspondence: suqiao@fio.org.cn

**Abstract:** This study investigated the hydrochemical characteristics and formation mechanism of natural water in the southeastern Qinghai-Tibet Plateau. To this end, 19 groundwater samples were collected, tested, and analyzed using various methods, such as mathematical statistics, a Piper diagram, correlation analysis, Gibbs plots, and an ion ratio analysis. The results show that the dominant anions are  $\text{HCO}_3^-$  and  $\text{SO}_4^{2-}$ , and the dominant cations are  $\text{Ca}^{2+}$  and  $\text{Mg}^{2+}$ , which accounted for 98.50% and 85.94% of the total amount of anions and cations, respectively. The samples were weakly alkaline water, where the TDS (total dissolved solids) ranged from 28.00 mg/L to 242.00 mg/L, with an average value of 129.10 mg/L. The hydrochemical types were mainly Ca-Mg- $\text{HCO}_3$ - $\text{SO}_4$ —accounting for 42.10%. The hydrochemical evolution process was found to be mainly controlled by the weathering and dissolution of carbonate and silicate rocks. The main sources of  $\text{Na}^+$  and  $\text{K}^+$  are rock salt and silicate rocks, and those of  $\text{Ca}^{2+}$ ,  $\text{Mg}^{2+}$ ,  $\text{HCO}_3^-$ , and  $\text{SO}_4^{2-}$  are from the dissolution of dolomite, calcite, gypsum, and other calcium and magnesium bearing minerals. In addition, atmospheric precipitation serves as a replenishment source of natural water in the region, and the recharge is affected by evaporation.

**Keywords:** natural water; hydrochemical characteristics; cause analysis; southeastern Qinghai-Tibet plateau



**Citation:** Gao, Z.; Tong, H.; Su, Q.; Liu, J.; Gao, F.; Han, C. Hydrochemical Characteristics and Cause Analysis of Natural Water in the Southeast of Qinghai-Tibet Plateau. *Water* **2021**, *13*, 3345. <https://doi.org/10.3390/w13233345>

Academic Editor: Pankaj Kumar

Received: 22 October 2021

Accepted: 22 November 2021

Published: 25 November 2021

**Publisher's Note:** MDPI stays neutral with regard to jurisdictional claims in published maps and institutional affiliations.



**Copyright:** © 2021 by the authors. Licensee MDPI, Basel, Switzerland. This article is an open access article distributed under the terms and conditions of the Creative Commons Attribution (CC BY) license (<https://creativecommons.org/licenses/by/4.0/>).

## 1. Introduction

Water resources are not only necessary for life sustenance, but also an important strategic resource for supporting national, social, and economic development; moreover, they play an important role in maintaining ecological balance [1,2]. The chemical composition of natural water bodies is affected by many factors, such as the geological structure, climate, recharge type, topography, hydrogeological conditions, rock types, and the degree of weathering. However, the key factors affecting the hydrochemical composition of water bodies are widely variable across different regions. The geochemical environment and evolution history of a region can be ascertained by analyzing the chemical composition of its water resources, thereby providing a theoretical basis for the scientific and rational development of water resources in the region [3–5]. The Qinghai-Tibet Plateau is sensitive and fragile, owing to its high-altitude environment, and its hydrochemical characteristics significantly affect its ecological environment. A proper understanding of the chemical components of water in this area and their mechanisms is of great significance for maintaining ecological balance, and scientifically and rationally developing and utilizing water resources.

The Qinghai-Tibet Plateau, as the birthplace of the Yangtze River, Yellow River, Nu River, and other major rivers, is even more of a hot spot. Many scholars have conducted

research on the hydrochemistry of the region. Zhang et al. [6] discussed the characteristics and mechanisms of the chemistry of the Niyang River and found that the water chemical composition of the basin is controlled by the weathering and dissolution of silicate and carbonate rocks. Wang et al. [7] studied the Ne isotopes of surface water and groundwater in the eastern part of the Qinghai-Tibet Plateau and found that the Ne content in this area has a low zonal pattern in the southeast, and a high one in the west and north. Liu et al. [8] studied the stable isotopes of different water bodies in the Lhasa River Basin. Zhang et al. [9] studied the hydrochemical characteristics and sources of main ions in the Lhasa River Basin and found that the concentration of main ions follows the order winter > spring > autumn > summer, with a negative correlation between the concentration of main ions and river runoff. Tian et al. [10] studied the regional differences in the natural water chemistry and their causes in the western, southern, and northeastern border regions of the Qinghai-Tibet Plateau, which are affected by human activities. Due to the influence of many factors, such as high altitude, bad weather, and inconvenient transportation, people have performed relatively little research on the Qinghai-Tibet Plateau. However, the current research is mainly focus on relatively small spatial scales, and relatively little research has been conducted on large spatial scales. This study attempts to analyze the hydrochemical characteristics and formation mechanism of natural water in the southeast of the Qinghai-Tibet Plateau through statistical analysis, a Piper diagram, a Gibbs diagram, and an ion ratio analysis, which explain the hydrochemical characteristics and causes of the natural water in this area to a certain extent, and supplement and update the research data in this area.

## 2. Study Area

The study area is located in the southeast of the Qinghai-Tibet Plateau, between  $29^{\circ}14'53''$ – $32^{\circ}18'54''$  N and  $90^{\circ}37'34''$ – $97^{\circ}36'29''$ . There are high and steep mountains, steep and deep gullies, and plateau hills in the area. Under the influence of topography, landform, and atmospheric circulation, the study areas have unique characteristics with complex terrain and highly variable weather. The climate is generally cold and dry in the northwest and warm and humid in the southeast. The climate in the region can be further divided into several zones: a sub-frigid climate zone; a sub-temperate, sub-humid plateau climate zone; a temperate, semi-arid monsoon plateau climate zone; and a tropical humid and a semi-humid climate zone. The area experiences distinct dry and rainy seasons, with the rainy season during May–September accounting for approximately 90% of the annual rainfall. Furthermore, rainfall is highly uneven in terms of spatial distribution. The study area has many rivers, and the major rivers are the Nu River, Niyang River, and Lhasa River.

Geologically, the study area is generally located in the Gangdese-Himalayan orogenic system, and a very small part is located in the Bangong-Shuanghu-Nuijiang-Jiangning docking zone [11]. Since the Paleozoic, strata have been fully developed and the sedimentary types are diverse. The study area has complex rock types with well-exposed Mesozoic and Cenozoic marine strata and widely distributed igneous and metamorphic rocks [12].

## 3. Materials and Methods

### 3.1. Sampling and Analysis

In this study, 19 natural water samples were collected from September 2020 to October 2020, and the locations of the sampling points are shown in Figure 1. The sampling process is as follows. First, 1 L polyethylene bottles were washed with the water to be tested 2–3 times, and then dried before collecting the samples. After sampling and ensuring that no bubbles were present, the bottles were sealed to prevent leakage. The samples were sent to the laboratory for testing as soon as possible. A portable water quality parameter instrument HD40D (Hach, Loveland, CO, USA) was used on site to measure pH, total dissolved solids (TDS), and electrical conductivity (EC). The  $\text{Na}^+$  and  $\text{K}^+$  ions were determined by flame atomic absorption spectrophotometry with a detection limit of 2.0 mg/L. The instrument was an atomic absorption spectrophotometer. The levels

of  $\text{Ca}^{2+}$  and  $\text{Mg}^{2+}$  were determined by EDTA titration, wherein the detection limit was 0.01 mg/L.  $\text{HCO}_3^-$  levels were measured by acid-base titration, and the detection limit was 1.0 mg/L. The  $\text{SO}_4^{2-}$ ,  $\text{Cl}^-$  and  $\text{NO}_3^-$  levels, which were detected by ion chromatography with corresponding detection limits of 0.09 mg/L, 0.02 mg/L, and 0.2 mg/L, respectively. The instrument used was an ion chromatograph ICS-2100 produced by the DIONEX company in the United States. Fe, Mn, Zn, Cu, Cr and Co were all detected by inductively coupled plasma mass spectrometry, and the corresponding detection limits were 5 ng/mL, 2 ng/mL, 2 ng/mL, 4 ng/mL, 10 ng/mL, and 2 ng/mL, respectively. The instrument used was an inductively coupled plasma mass spectrometer (iCAP PQ) produced by Thermo Fisher Scientific. The hydrogen and oxygen isotopes were measured by stable isotope mass spectrometry (MAT253Plus, Thermo Scientific, Dreieich, Germany). During the testing process, quality control was carried out, and blank value determination was carried out for all measured parameters. Additionally, parallel sample determination and standard sample determination were carried out for 5 samples in each experimental interval to ensure the accuracy and validity of the experimental data. For all determinations, the anion and cation charge balance test was conducted through the Formula (1), and the charge balance error of the test data was less than 5% of the standard, indicating the accuracy and reliability of the test results [13].

$$E(\%) = \frac{\sum N_c - \sum N_b}{\sum N_c + \sum N_b} \times 100\% \quad (1)$$

where E is the relative error of anions and cations, and  $N_c$  and  $N_b$  are the milliequivalent concentrations of anions and cations, meq/L.

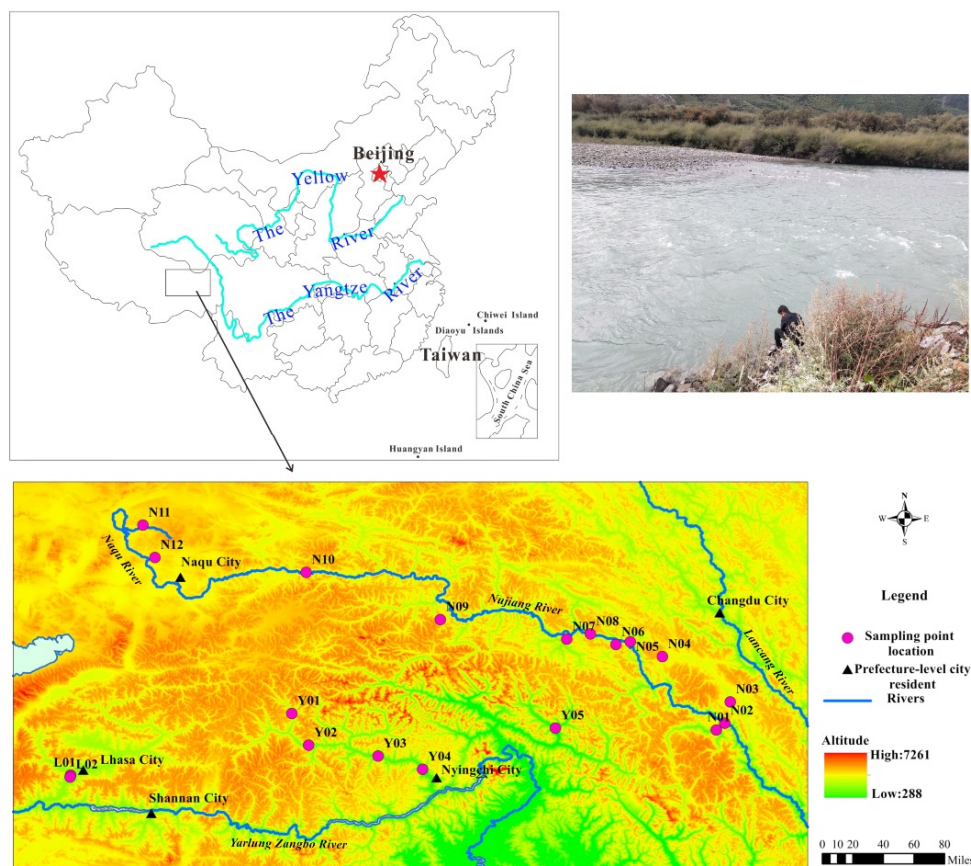


**Figure 1.** Geographical location and distribution of sampling points in the study area.

### 3.2. Analysis of Hydrogeochemical Processes

Statistical analysis and Pearson correlation analysis on the maximum (Max), minimum (Min), average (Mean), standard deviation (SD), and coefficient of variation (CV) of each index were performed in SPSS 22.0. The Piper plots were drawn using AQQA software, and water samples were classified using the Shukarev classification method. Correlation analysis was performed using the Gibbs model, and the main controlling factors of the natural water chemistry were explored using the ion ratio method.

## 4. Results and Discussion

### 4.1. Statistical Analysis

#### 4.1.1. Hydrochemical Characteristics

Table 1 and Figure 2, respectively, show the statistical results and box diagram of the hydrochemical characteristic parameters of the natural water in the study area. China and World Health Organization drinking water standards are also listed in Table 1 for easy evaluation and comparison [14,15]. The heavy metals, such as Fe, Mn, Zn, Cu, Cr, Co, etc., in the water samples are not detected, or the content is very small and can be ignored. The cation content followed the order  $\text{Ca}^{2+} > \text{Mg}^{2+} > \text{Na}^+ > \text{K}^+$ , and their average mass concentrations were 34.39 mg/L, 12.07 mg/L, 6.32 mg/L, and 1.27 mg/L, respectively. Accounting for approximately 85.94% of the total cations,  $\text{Ca}^{2+}$  and  $\text{Mg}^{2+}$  are the dominant cations. The anion content followed the order  $\text{HCO}_3^- > \text{SO}_4^{2-} > \text{Cl}^- > \text{NO}_3^-$ , and their average mass concentrations were 133.43 mg/L, 45.65 mg/L, 1.47 mg/L, and 1.26 mg/L, respectively. Accounting for approximately 98.50% of the total anions,  $\text{HCO}_3^-$  and  $\text{SO}_4^{2-}$  are the dominant anions. The content of  $\text{NO}_3^-$  was low, indicating weak influence of human activities. The pH value of the natural water samples in the study area was between 7.57 and 8.30, with an average value of 7.87. The overall pH value was weakly alkaline, and its coefficient of variation was 0.03, indicating a small spatiotemporal variation of pH. The range of EC was between 53.50 and 449.00  $\mu\text{S}/\text{cm}$ , with an average value of 241.31  $\mu\text{S}/\text{cm}$ . The variation range of TDS was between 28.0 and 242.0 mg/L, and the average value was 129.10 mg/L. After dividing brackish water according to the TDS, fresh water and brackish water accounted for 36.8% and 63.2% of the total water samples, respectively. Hardness (the equivalent of  $\text{CaCO}_3$ ) was calculated by multiplying the total number of milligrams of Ca and Mg by 50. In terms of hardness, water was classified into the following types: very soft water (less than 75 mg/L), soft water (75–150 mg/L), medium hard water (150–300 mg/L), hard water (300–450 mg/L), and extremely hard water (greater than 450 mg/L). The hardness of the natural water samples in the study area was between 30.85 and 256.30 mg/L, with an average of 136.24 mg/L, and the extremely soft water, soft water, and medium–hard water samples accounted for 31.58%, 26.32%, and 42.10% of the total water samples, respectively. Hard water and extremely hard water were not observed. The concentration of conventional ions, TDS, and other indicators in the study area are far less than the World Health Organization (WHO) [14] drinking water standards and China's drinking water sanitation standards [15], indicating that the water quality in the study area is very good and suitable for drinking.

**Table 1.** Mass concentration statistics of main hydrochemical indexes.

Number	K <sup>+</sup>	Na <sup>+</sup>	Ca <sup>2+</sup>	Mg <sup>2+</sup>	Cl <sup>-</sup>	HCO <sub>3</sub> <sup>-</sup>	SO <sub>4</sub> <sup>2-</sup>	NO <sub>3</sub> <sup>-</sup>	PH	TDS	EC	δD	δ <sup>18</sup> O
Y01	0.86	2.07	20.92	4.89	0.71	61.02	30.54	1.26	7.57	133	250	-146.15	-23.39
Y02	0.85	2.05	20.90	5.17	0.57	55.28	35.70	0.84	7.87	73.4	138.8	-140.90	-20.23
Y03	0.86	1.54	16.31	3.13	0.51	45.77	22.83	0.72	7.8	54.5	103.9	-129.25	-19.49
Y04	0.70	1.19	10.00	1.41	0.30	30.51	9.71	0.36	7.77	28	53.5	-119.22	-15.61
Y05	1.47	0.96	22.14	3.26	0.17	76.28	12.36	0.30	7.67	57.3	108.5	-118.76	-16.69
N01	1.09	7.46	30.64	5.27	1.25	100.79	39.19	0.76	7.6	101	190.2	-130.25	-17.30
N02	1.31	5.97	50.85	18.45	1.07	167.81	71.74	1.04	7.58	170	318	-136.87	-18.77
N03	0.98	3.36	32.59	9.25	0.62	122.30	34.30	0.93	7.73	109.1	205.2	-135.72	-18.23
N04	0.72	2.82	11.36	4.07	0.16	60.28	6.04	0.49	7.7	44	83.6	-135.75	-17.94
N05	0.93	2.63	45.50	20.17	0.60	208.83	37.37	1.29	7.71	168.5	315	-131.28	-16.42
N06	1.50	4.04	52.49	14.41	1.15	205.08	44.55	1.08	8.04	164.1	306	-130.62	-16.51

Table 1. Cont.

Number	K <sup>+</sup>	Na <sup>+</sup>	Ca <sup>2+</sup>	Mg <sup>2+</sup>	Cl <sup>-</sup>	HCO <sub>3</sub> <sup>-</sup>	SO <sub>4</sub> <sup>2-</sup>	NO <sub>3</sub> <sup>-</sup>	PH	TDS	EC	δD	δ <sup>18</sup> O
N07	0.85	3.96	26.43	11.12	0.84	96.79	47.29	0.81	8.02	106.5	200	-122.52	-15.83
N08	1.29	7.94	47.46	23.80	1.51	178.32	98.27	1.36	7.99	194.9	363	-126.83	-19.39
N09	0.58	3.42	40.87	36.99	0.24	106.79	174.34	0.77	7.94	223.0	411	-137.14	-19.53
N10	2.53	21.25	54.75	27.30	4.28	259.34	96.37	2.13	8.14	242.0	449	-115.09	-15.64
N11	2.00	13.17	55.02	10.88	2.57	254.59	16.31	3.48	8.30	170.7	319	-113.86	-16.85
N12	3.11	25.31	54.27	18.20	7.03	300.36	27.25	2.76	8.18	214.2	397	-116.18	-15.18
L01	1.22	5.55	30.08	5.72	2.24	102.04	31.46	1.74	8.14	99.4	186.7	-134.24	-17.66
L02	1.19	5.45	30.80	5.76	2.17	103.04	31.65	1.85	7.87	99.3	186.5	-135.08	-18.68
Min	0.58	0.96	10.00	1.41	0.16	30.51	6.04	0.30	7.57	28.00	53.50	-146.15	-23.39
Max	3.11	25.31	55.02	36.99	7.03	300.36	174.34	3.48	8.30	242.00	449.00	-113.86	-15.18
Mean	1.27	6.32	34.39	12.07	1.47	133.43	45.65	1.26	7.87	129.10	241.31	-129.25	-17.86
SD	0.63	6.50	14.95	9.49	1.65	78.07	39.23	0.80	0.21	62.44	115.02	9.07	1.97
CV	0.50	1.03	0.43	0.79	1.12	0.59	0.86	0.64	0.03	0.48	0.48	-0.07	-0.11
WHO	10	200	75	50	250	300	400	45	8.5	500			
CS		200			250	-	250	10	6.5–8.5	1000			

mg/L for ions and TDS;  $\mu\text{s}/\text{cm}$  for EC; pH and coefficient of variation are dimensionless; SD: standard deviation; CV: coefficient variation. WHO: drinking water standard specifications given by WHO (2017) [14]; CS: standards for drinking water quality of China [15].

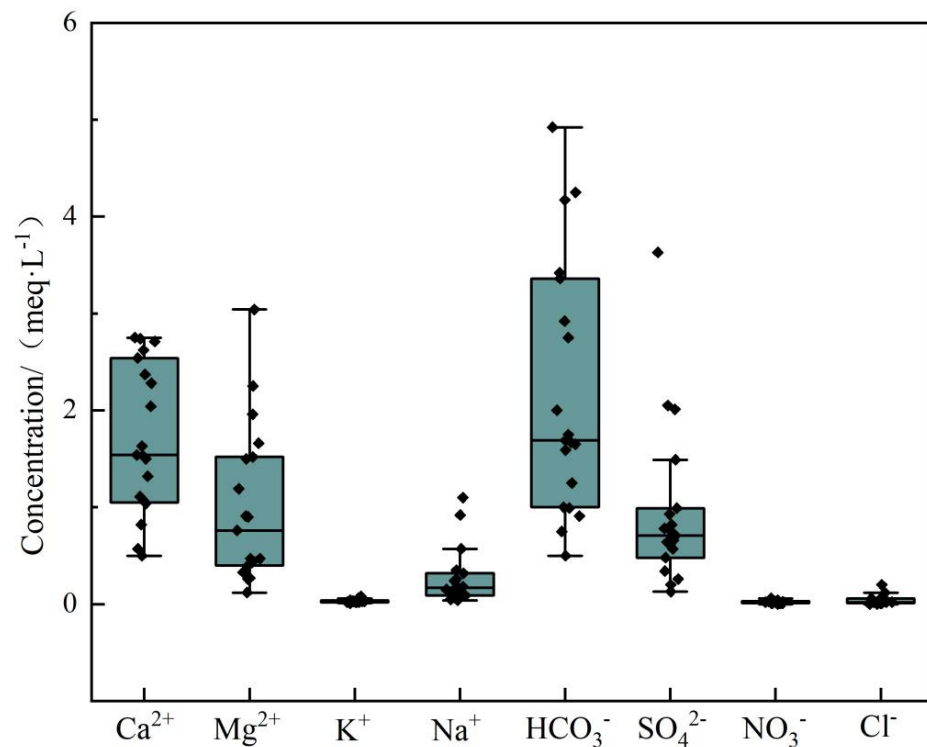
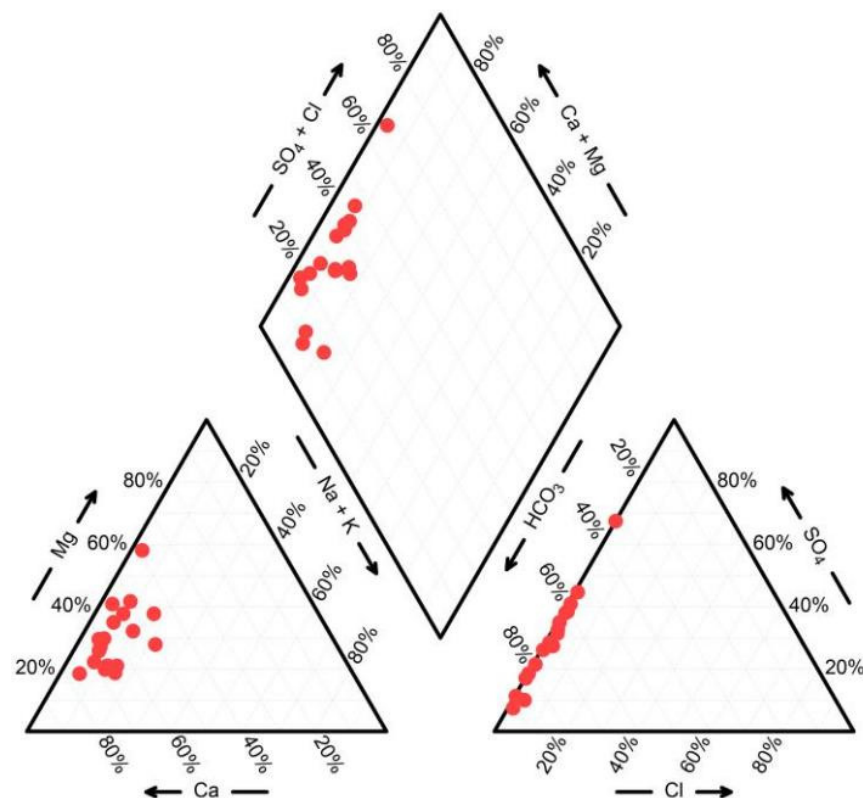


Figure 2. Box-plot of natural water chemical parameters.

#### 4.1.2. Hydrochemical Types

The Piper diagram [16,17] can intuitively reflect the ratio of the main ions in water and can be used to rapidly determine the water chemical phase of natural water. As shown in Figure 3, anions are distributed close to the HCO<sub>3</sub><sup>-</sup> axis and the Cl<sup>-</sup> content in the water body is low, indicating that the dominant anions in the study area are HCO<sub>3</sub><sup>-</sup> and SO<sub>4</sub><sup>2-</sup>; cations are distributed near the Ca<sup>2+</sup>–Mg<sup>2+</sup> end, indicating that Ca<sup>2+</sup> and Mg<sup>2+</sup> are the dominant cations. According to the Shukarev classification [18], the study area has four types of natural water, namely the Ca·Mg-HCO<sub>3</sub>·SO<sub>4</sub> type, Ca-HCO<sub>3</sub>·SO<sub>4</sub> type, Ca·Mg-HCO<sub>3</sub> type, and Ca-HCO<sub>3</sub> type. Among them, Ca·Mg-HCO<sub>3</sub>·SO<sub>4</sub> was the main type, accounting for 42.10% of the total water samples, followed by Ca-HCO<sub>3</sub>·SO<sub>4</sub> and Ca·Mg-HCO<sub>3</sub>, accounting for 26.3% and 21.1%, respectively.



**Figure 3.** Piper diagram of natural water chemistry.

#### 4.2. Cause Analysis of Hydrochemical Characteristics

##### 4.2.1. Gibbs Diagram

In the natural world, water bodies have various continuous hydrogeochemical interactions with the surrounding environment. Affected by various factors, the chemical composition and TDS concentration of water bodies change [4]. The Gibbs diagram is a tool for analyzing the main controls on the evolution of hydrochemical characteristics [19–22]. Based on the relationship between  $\text{Cl}^- / (\text{Cl}^- + \text{HCO}_3^-)$ ,  $\text{Na}^+ / (\text{Na}^+ + \text{Ca}^{2+})$ , and TDS, the processes controlling hydrochemistry are divided into evaporation, crystallization, rock weathering, and atmospheric precipitation [20]. The abscissa of the Gibbs diagram (Figure 4) corresponds to the ratio of anions and cations, and the ordinate to the logarithmic coordinate of TDS, namely  $\text{Na}^+ / (\text{Na}^+ + \text{Ca}^{2+})$  and  $\text{Cl}^- / (\text{Cl}^- + \text{HCO}_3^-)$ . The variation range of TDS in the study area was between 28.0 and 242.0 mg/L, the ratio of  $\text{Cl}^- / (\text{Cl}^- + \text{HCO}_3^-)$  was between 0.004 and 0.039, and the ratio of  $\text{Na}^+ / (\text{Na}^+ + \text{Ca}^{2+})$  was between 0.036 and 0.289. As shown in Figure 4, the natural water in the study area is mainly distributed in the rock weathering control area, indicating that rock weathering is the main factor controlling the hydrochemical characteristics of the natural water. This is basically consistent with the conclusions of other rivers in the world [23–25] and other scholars on rivers in the Qinghai-Tibet Plateau [26–29].

##### 4.2.2. Correlation Analysis

There is a certain relationship between the changes in the concentration of each ion in the water body. By studying the correlation, the source relationship between the ions can be inferred [30]. Table 2 shows that the TDS have a significant positive correlation with the eight conventional ions. Among them, the correlation coefficients of the TDS with  $\text{HCO}_3^-$ ,  $\text{Mg}^{2+}$ , and  $\text{Ca}^{2+}$  were greater than 0.8, indicating that these three ions are the main factors controlling the level of TDS.  $\text{Cl}^-$  showed a strong correlation with  $\text{Na}^+$  and  $\text{K}^+$ , with correlation coefficients of 0.953 and 0.919, respectively, indicating that these three ions have a common source, which may be the weathering and dissolution of evaporites (KCl

and NaCl). The correlation coefficient of  $Mg^{2+}$  and  $SO_4^{2-}$  was 0.883, indicating that their common source may be the dissolution of sulfur-containing minerals such as gypsum.

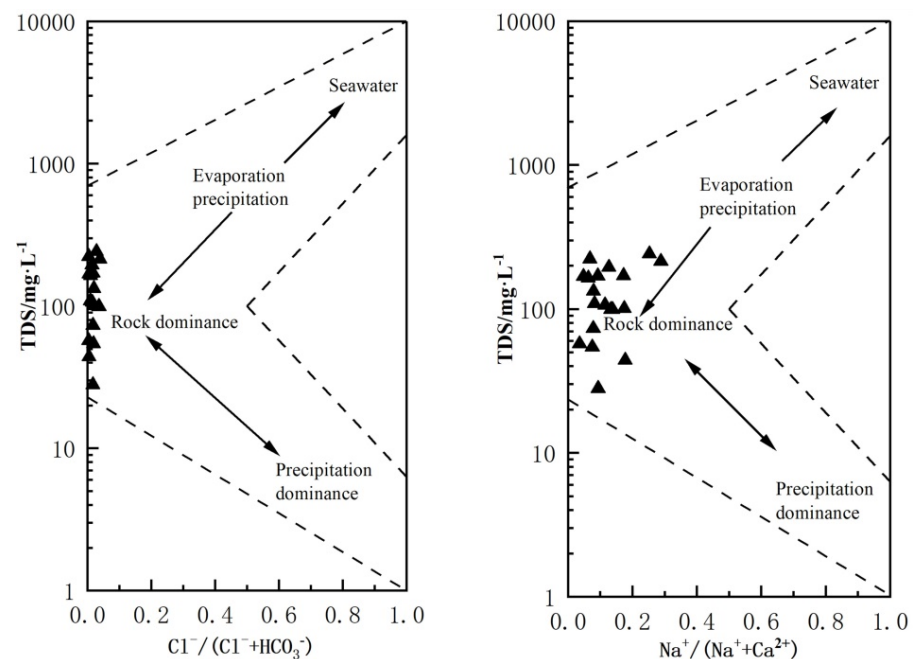


Figure 4. Gibbs plots for natural water in the study area.

Table 2. Correlation coefficients among various water chemical parameters of the natural water.

	Na <sup>+</sup>	HCO <sub>3</sub> <sup>-</sup>	K <sup>+</sup>	Mg <sup>2+</sup>	Ca <sup>2+</sup>	Cl <sup>-</sup>	SO <sub>4</sub> <sup>2-</sup>	NO <sub>3</sub> <sup>-</sup>	TDS
Na <sup>+</sup>	1								
HCO <sub>3</sub> <sup>-</sup>	0.815 **	1							
K <sup>+</sup>	0.926 **	0.830 **	1						
Mg <sup>2+</sup>	0.418	0.594 **	0.281	1					
Ca <sup>2+</sup>	0.669 **	0.933 **	0.677 **	0.724 **	1				
Cl <sup>-</sup>	0.953 **	0.751 **	0.919 **	0.285	0.590 **	1			
SO <sub>4</sub> <sup>2-</sup>	0.146	0.213	-0.031	0.883 **	0.448	0.014	1		
NO <sub>3</sub> <sup>-</sup>	0.768 **	0.770 **	0.746 **	0.257	0.675 **	0.780 **	-0.016	1	
TDS	0.660 **	0.820 **	0.570 *	0.890 **	0.900 **	0.560 **	0.687 **	0.581 **	1

\*\* indicates a significant correlation at the 0.01 level; \* indicates a significant correlation at the 0.05 level.

#### 4.2.3. Ion Ratio

Using the relationship between  $\gamma Ca^{2+} / \gamma Na^{+}$ ,  $\gamma Mg^{2+} / \gamma Na^{+}$ , and  $\gamma HCO_3^{-} / \gamma Na^{+}$ , the influence of rock weathering types on the chemical composition of the natural water in the area can further be judged [31]. Figure 5 shows that the sampling points are distributed between silicate rocks and carbonate rocks, with higher inclination towards carbonate rocks. According to this distribution, the hydrochemical characteristics of the natural water in the study area are jointly controlled by the weathering and dissolution of carbonate and silicate rocks, with carbonates having stronger influence than silicates.

In the chemical composition of the water, the difference in the content ratio between the components can be used to reflect the cause of the water chemistry [32,33]. A water sample point near  $(Na^{+} + K^{+}) / Cl^{-} = 1$  indicates that the dissolution of evaporative rock salt plays a major role [34]. In Figure 6a, the water sample points are all above the 1:1 contour, indicating that the  $Cl^{-}$  content is not high enough to reach equilibrium with  $Na^{+}$  and  $K^{+}$ , and it is generally believed that  $K^{+}$  and  $Na^{+}$  originate from the weathering dissolution of silicate rocks or evaporites [35,36]. Therefore, the excess  $Na^{+}$  and  $K^{+}$  may be attributable to the weathering of silicate minerals.

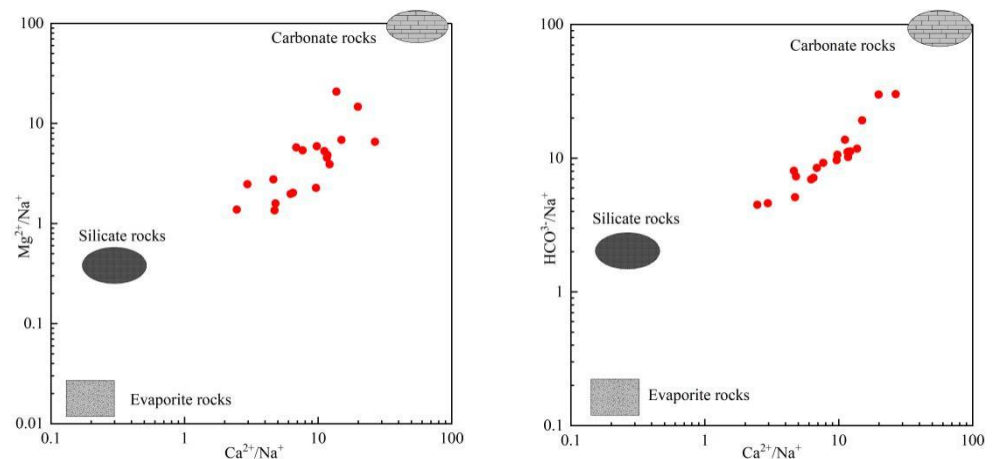


**Figure 5.** Relative contribution of weathering and dissolution of rocks.

$\text{Ca}^{2+}$  and  $\text{Mg}^{2+}$  in the natural water may originate from the dissolution of evaporites, silicates, or carbonates containing calcium and magnesium. Using the milligram equivalent ratio of  $(\text{Ca}^{2+} + \text{Mg}^{2+})$  and  $(\text{HCO}_3^- + \text{SO}_4^{2-})$ , the main sources of  $\text{Mg}^{2+}$  and  $\text{Ca}^{2+}$  can be ascertained [37,38]. As shown in Figure 6b, most of the sample points fall near or below the  $\gamma(\text{Ca}^{2+} + \text{Mg}^{2+})/\gamma(\text{HCO}_3^- + \text{SO}_4^{2-}) = 1$  contour, indicating that the  $\text{Ca}^{2+}$  and  $\text{Mg}^{2+}$  originate from the weathering dissolution of silicate rocks and evaporites, and the weathering dissolution of carbonates. The ratio of  $\gamma(\text{Ca}^{2+} + \text{Mg}^{2+})$  and  $\gamma(\text{HCO}_3^-)$  can be used to further understand the source of  $\text{Ca}^{2+}$  and  $\text{Mg}^{2+}$ . Figure 6c shows that most of the sample points fall on the upper left of the 1:1 contour, indicating that the weathering and dissolution of carbonate rocks dominate the chemical components. At the same time, the  $\text{Mg}^{2+}$  equivalent concentration ratios of  $\text{Ca}^{2+}/\text{SO}_4^{2-}$  and  $\text{Mg}^{2+}/\text{SO}_4^{2-}$  at sample points—except one point—are greater than 1, indicating that the  $\text{Mg}^{2+}$  has a higher content than  $\text{Ca}^{2+}$ . In other words, the contribution of carbonate weathering is higher than that of sulfates [39]. The ratio of  $(\text{Ca}^{2+} + \text{Mg}^{2+})/(\text{Na}^+ + \text{K}^+)$  in water bodies can be used to judge the weathering intensity of different types of rocks [40]; higher ratios of  $\gamma(\text{Ca}^{2+} + \text{Mg}^{2+})/\gamma(\text{Na}^+ + \text{K}^+)$  suggest the dominance of salt weathering and dissolution control, whereas lower ratios suggest evaporite weathering. In the water samples, the ratio of  $\gamma(\text{Ca}^{2+} + \text{Mg}^{2+})/\gamma(\text{Na}^+ + \text{K}^+)$  was large (Figure 6d), ranging from 3.58 to 31.32 with an average value of 12.36, indicating that the main cations originate from the weathering dissolution of carbonates.

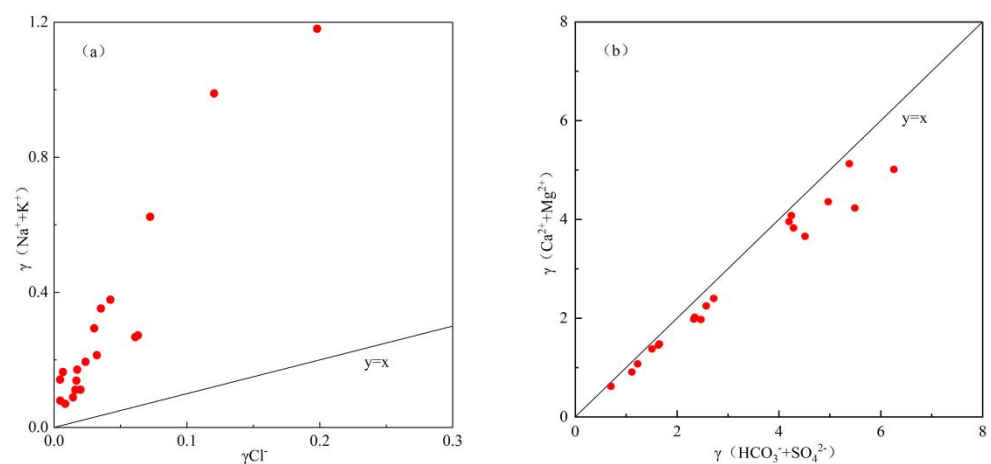


**Figure 6.** Cont.

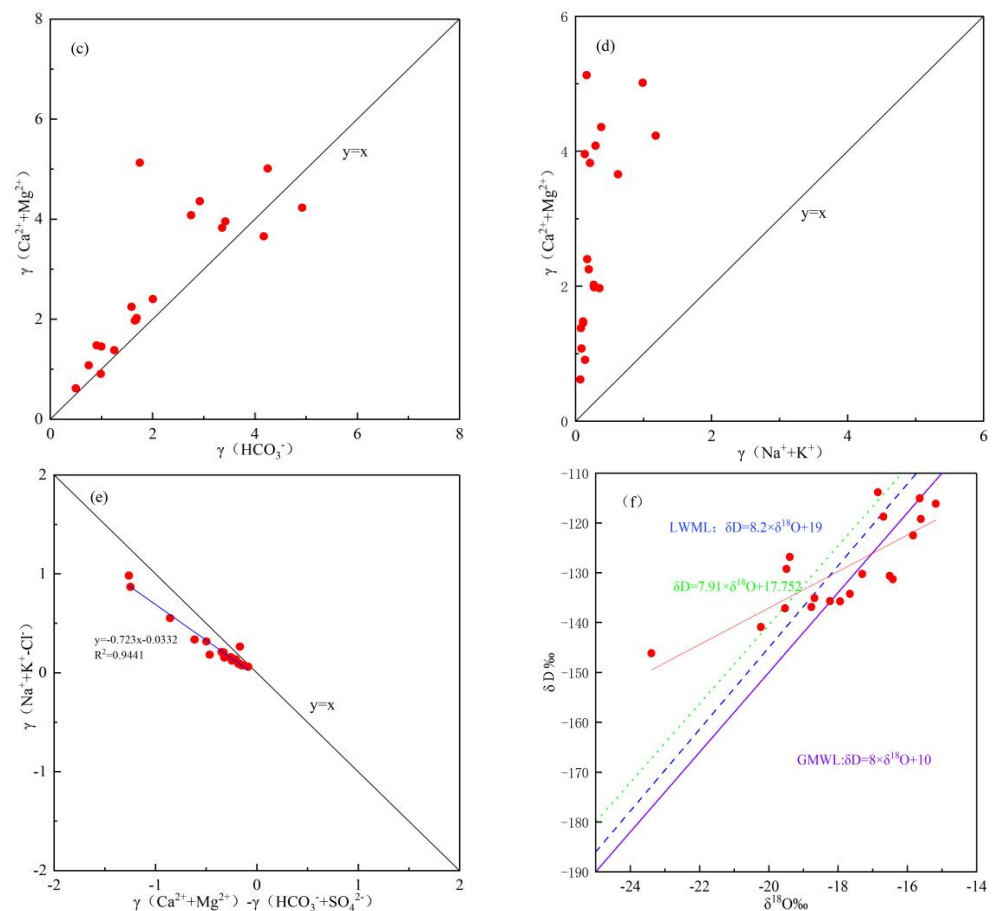


**Figure 6.** The ratio diagram of main ions in the natural water in the study area (a)  $\gamma(\text{Na}^+ + \text{K}^+)/\gamma(\text{Cl}^-)$ ; (b)  $\gamma(\text{Ca}^{2+} + \text{Mg}^{2+})/\gamma(\text{HCO}_3^- + \text{SO}_4^{2-})$ ; (c)  $\gamma(\text{Ca}^{2+} + \text{Mg}^{2+})/\gamma(\text{HCO}_3^-)$ ; (d)  $\gamma(\text{Ca}^{2+} + \text{Mg}^{2+})/\gamma(\text{Na}^+ + \text{K}^+)$ ; (e)  $\gamma[(\text{Na}^+ + \text{K}^+) - \text{Cl}^-]/[\gamma(\text{Ca}^{2+} + \text{Mg}^{2+}) - \gamma(\text{HCO}_3^- + \text{SO}_4^{2-})]$ ; (f)  $\delta\text{D}/\delta^{18}\text{O}$ .

The sources of solutes can be approximated from the ratio of  $\text{Mg}^{2+}/\text{Ca}^{2+}$  and  $\text{Na}^+/\text{Ca}^{2+}$ . In general, the ratio of  $\text{Na}^+/\text{Ca}^{2+}$  and  $\text{Mg}^{2+}/\text{Ca}^{2+}$  in water dominated by calcite dissolution is relatively low, while the ratio of  $\text{Mg}^{2+}/\text{Ca}^{2+}$  in water dominated by dolomite weathering and dissolution is high (about 1) and is higher than the  $\text{Na}^+/\text{Ca}^{2+}$  ratio. Under normal temperature conditions, when dolomite and calcite dissolution are balanced, the value of  $\text{Mg}^{2+}/\text{Ca}^{2+}$  is approximately 0.8 [41]. The average values of the ratios of  $\text{Na}^+/\text{Ca}^{2+}$  and  $\text{Mg}^{2+}/\text{Ca}^{2+}$  in the natural water were low at 0.14 and 0.53, respectively, indicating that the dissolution of calcite minerals is the main source of ions in the natural water in this area. Cation exchange also plays an important role in the chemical composition of natural water. The exchange of cations can be assessed from the ratio of  $\gamma(\text{Na}^+ + \text{K}^+) - \text{Cl}^-$  and  $\gamma(\text{Ca}^{2+} + \text{Mg}^{2+}) - \gamma(\text{HCO}_3^- + \text{SO}_4^{2-})$  [42]. Figure 6e shows that the sample points are distributed around a straight line with a slope of  $-0.723$  and  $R^2$  is 0.9441, indicating the occurrence of cation exchange—but it is not the main factor affecting the chemical composition of water.

#### 4.3. Isotopic Characteristics

Stable hydrogen and oxygen isotopes are an important basis for studying the evolution and source of water bodies. In this study, the value of  $\delta\text{D}$  was between  $-146.15\%$  and  $-133.86\%$ , with an average value of  $-129.25\%$ ; the value of  $\delta^{18}\text{O}$  was between  $-23.39\%$  and  $-15.18\%$ , with an average value of  $-17.86\%$ . The local atmospheric precipitation line (LWML) in this study coincided with the atmospheric precipitation line in the eastern Qinghai-Tibet Plateau proposed by Yu et al. [43]:  $\delta\text{D} = 8.2\delta^{18}\text{O} + 19$ . The distribution of data points of  $\delta\text{D}$  and  $\delta^{18}\text{O}$  on the scatter diagram (Figure 6f) was analyzed. According to the measured data of the water samples, the fitting curve of the natural water in the

study area was fitted as follows:  $\delta D = 3.66\delta^{18}O - 63.86$  ( $R^2 = 0.63$ ). Compared with the global atmospheric precipitation line (GMWL)  $\delta D = 8\delta^{18}O + 10$  proposed by Craig [44], the atmospheric precipitation line  $\delta D = 7.91\delta^{18}O + 17.752$  proposed by Qin et al. [45], and the local atmospheric precipitation, most of the sample points are distributed below or near LWML, with a small deviation, indicating that the water bodies in the study area are mainly derived from atmospheric precipitation during summer. The distribution of hydrogen and oxygen isotopes in the water body along the atmospheric precipitation line is affected by various factors, such as elevation, temperature, continental effect, precipitation, and latitude, which lead to deviations [46]. The slope of the fitted natural water curve was 3.66, which is smaller than the slope of the atmospheric precipitation line in this area, indicating that the hydrogen and oxygen stable isotopes of natural water are affected by evaporation [47].

## 5. Conclusions

The Qinghai-Tibet Plateau is an ecologically fragile area with low temperatures, and water resources are of great significance to maintaining its ecological balance. In this study, based on field sampling, the chemical characteristics of natural water in the area were explored and the causes were analyzed by various methods.

The average pH of the natural water in the study area is 7.87, which is weakly alkaline as a whole; the average TDS is 129.10 mg/L, and the maximum does not exceed 242 mg/L. The concentration of each main ion is kept at a low level, and the concentration of  $\text{Na}^+$  and  $\text{Cl}^-$  is extremely low, basically less than 1 mol/L.

The Piper diagram shows that the dominant cations are  $\text{Ca}^{2+}$  and  $\text{Mg}^{2+}$ , and the anions are  $\text{HCO}_3^-$  and  $\text{SO}_4^{2-}$ . According to the Shukarev classification, there are four types of water chemistry, the Ca-Mg- $\text{HCO}_3$ - $\text{SO}_4$  type, the Ca- $\text{HCO}_3$ - $\text{SO}_4$  type, the Ca-Mg- $\text{HCO}_3$  type, and the Ca- $\text{HCO}_3$  type, of which the Ca-Mg- $\text{HCO}_3$ - $\text{SO}_4$  type accounted for 42.1% of the total.

Through the Gibbs diagram and main ion ratio diagram, it is concluded that the hydrochemical composition of the natural water in the study area mainly comes from the weathering dissolution of carbonate rock and silicate rock, and the influence of weathering of carbonate rock on hydrochemical composition is greater than that of silicate rock.

Analyzing the  $\delta D$  and  $\delta^{18}O$  isotopes of the natural water in the study area with GMWL and LWML, the main source of replenishment was found to be atmospheric precipitation, and it is affected by evaporation.

This study conducted a preliminary analysis of the chemical characteristics of natural water in the Qinghai-Tibet Plateau. It is believed that it is suitable for drinking. However, its water quality will change if it is affected by human activities. Therefore, long-term monitoring is required in future studies to ensure the natural water quality is good. In addition, there is often a close relationship between surface water and groundwater. In the future, it is necessary to conduct research on the interaction between surface water and groundwater in the Qinghai-Tibet Plateau.

**Author Contributions:** Conceptualization, H.T. and Z.G.; methodology, H.T., J.L. and C.H.; software, H.T. and F.G.; validation, H.T., Q.S. and Z.G.; formal analysis, H.T. and Z.G.; investigation, H.T. and J.L.; resources, Q.S., J.L. and Z.G.; data curation, H.T. and Z.G.; writing—original draft preparation, H.T. and Z.G.; writing—review and editing, Q.S. and C.H.; supervision, Q.S., J.L. and Z.G.; project administration, Q.S.; funding acquisition, Q.S., J.L. and Z.G. All authors have read and agreed to the published version of the manuscript.

**Funding:** This research was funded by China Postdoctoral Science Foundation (2020M682207) and General project of Shandong Natural Science Foundation (ZR2020MD109; ZR2020MD078).

**Data Availability Statement:** The data used in this paper is available from the corresponding author upon reasonable request.

**Acknowledgments:** The authors give their most sincere thanks to the editors and reviewers for their contributions to the improvement of this article.

**Conflicts of Interest:** The authors declare no conflict of interest.

## References

- Li, P.Y.; Qian, H. Water resources research to support a sustainable China. *Int. J. Water Resour. Dev.* **2018**, *34*, 327–336. [\[CrossRef\]](#)
- Hao, A.; Zhang, Y.; Zhang, E.; Li, Z.; Yu, J.; Wang, H.; Yang, J.; Wang, Y. Review: Groundwater resources and related environmental issues in China. *Hydrogeol. J.* **2018**, *26*, 1325–1337. [\[CrossRef\]](#)
- Ren, X.Z.; Li, J.G.; Liu, M.; Li, J.Y. Hydrochemical composition of natural waters and its affecting factors in the East Hunshandak Sandy Land. *Arid. Zone Res.* **2019**, *36*, 791–800. (In Chinese)
- Xing, L.N.; Guo, H.M.; Zhan, Y.H. Groundwater hydrochemical characteristics and processes along flow paths in the North China Plain. *J. Asian Earth Sci.* **2013**, *70*, 250–264. [\[CrossRef\]](#)
- Houria, B.; Mahdi, K.; Zohra, T.F. Hydrochemical characterisation of groundwater quality: Merdja plain (Tebessa town, Algeria). *Civ. Eng. J.* **2020**, *6*, 318–325. [\[CrossRef\]](#)
- Zhang, T.; Cai, W.T.; Li, Y.Z.; Zhang, Z.Y.; Geng, T.T.; Bian, C.; Zhao, M.; Cai, Y.M. Major ionic features and their possible controls in the water of the Niyang River Basin. *Environ. Sci.* **2017**, *38*, 4537–4545.
- Wang, S.L.; Li, Z.F.; Liu, J.S.; Liang, Z.X. Study on neon isotopes in surface water and groundwater in the eastern part of the Qinghai-Tibet Plateau. *Environ. Sci.* **1990**, *11*, 23–27. (In Chinese)
- Liu, J.T.; Gao, Z.J.; Wang, M.; Li, Y.Z.; Yu, C.; Shi, M.J.; Zhang, H.Y.; Ma, Y.Y. Stable isotope characteristics of different water bodies in the Lhasa River Basin. *Environ. Earth Sci.* **2019**, *78*, 71. [\[CrossRef\]](#)
- Zhang, Q.H.; Sun, P.A.; He, S.Y.; Wen, H.; Liu, M.L.; Yu, S. Chemical characteristics and sources of main ions in the river water of Lhasa River Basin in Tibet. *Environ. Sci.* **2018**, *39*, 1065–1075. (In Chinese)
- Tian, Y.; Yu, C.; Zha, X.; Gao, X.; Dai, E. Hydrochemical characteristics and controlling factors of natural water in the border areas of the Qinghai-Tibet Plateau(Article). *J. Geogr. Sci.* **2019**, *29*, 1876–1894. [\[CrossRef\]](#)
- Pan, G.T.; Wang, L.Q.; Zhang, W.P.; Wang, B.D. *The Geotectonic Map and Instructions of the Qinghai-Tibet Plateau and Adjacent Areas (1:1,500,000)*; Geological Publishing House: Beijing, China, 2013. (In Chinese)
- Lu, Y.; Li, Y.B.; Mima, P.C.; Hao, J.T.; Dexi, Z.Y. Evolution of structural geology and metallogenic unite, Xizang (Tibet) Autonomous Region. *Geol. Rev.* **2016**, *62*, 219–220. (In Chinese)
- Zhang, J.; Zhou, J.L.; Nai, W.H.; Zeng, Y.Y.; Chen, Y.F.; Wei, X. Spatial distribution and cause of shallow groundwater salinization in the plain area of the Yeerqiang River Basin in Xinjiang. *J. Agric. Eng.* **2019**, *35*, 135–143. (In Chinese)
- World Health Organization. *Guidelines for Drinking-Water Quality*; World Health Organization: Geneva, Switzerland, 2011.
- Ministry of Health of the PRC; Standardization Administration of the PRC. *Standards for Drinking Water Quality (GB5749–2006)*; China Standard: Beijing, China, 2006; (In Chinese).
- Piper, A.M. A graphic procedure in the geochemical interpretation of water-analyses. *Trans. Am. Geophys. Union* **1944**, *25*, 914–928. [\[CrossRef\]](#)
- Ebrahimi, M.; Kazemi, H.; Ehtashemi, M.; Rockaway, T.D. Assessment of groundwater quantity and quality and saltwater intrusion in the Damghan basin, Iran. *Geochemistry* **2016**, *76*, 227–241. [\[CrossRef\]](#)
- Reddy, A.G.S.; Kumar, K.N. Identification of the hydrogeochemical processes in groundwater using major ion chemistry: A case study of Penna-Chitravathi river basins in Southern India. *Environ. Monit. Assess.* **2010**, *170*, 365–382. [\[CrossRef\]](#)
- Tian, Y.; Yu, C.Q.; Luo, K.L.; Zha, X.J.; Wu, J.S.; Zhang, X.Z.; Ni, R.X. Hydrochemical characteristics and element contents of natural waters in Tibet, China. *J. Geogr. Sci.* **2015**, *25*, 669–686. [\[CrossRef\]](#)
- Gibbs, R.J. Mechanisms controlling world water chemistry. *Science* **1970**, *170*, 1088–1090. [\[CrossRef\]](#)
- Aref, F.; Roosta, R. Assessment of groundwater quality and hydrochemical characteristics in Farashband plain, Iran. *Arab. J. Geosci.* **2016**, *9*, 752. [\[CrossRef\]](#)
- Redwan, M.; Abdel Moneim, A.A. Factors controlling groundwater hydrogeochemistry in the area west of Tahta, Sohag, Upper Egypt. *J. Afr. Earth Sci.* **2016**, *118*, 328–338. [\[CrossRef\]](#)
- Stallard, R.F.; Edmond, J.M. Geochemistry of the Amazon: 3. Weathering chemistry and limits to dissolved inputs. *J. Geophys. Res. Part C Ocean.* **1987**, *92*, 8293–8302. [\[CrossRef\]](#)
- Qaisar, F.U.R.; Zhang, F.; Pant, R.R.; Wang, G.X.; Khan, S.; Zeng, C. Spatial variation, source identification, and quality assessment of surface water geochemical composition in the Indus River Basin, Pakistan. *Environ. Sci. Pollut. Res.* **2018**, *25*, 12736–12749. [\[CrossRef\]](#)
- Wu, H.W.; Wu, J.L.; Li, J.; Fu, C.S. Spatial variations of hydrochemistry and stable isotopes in mountainous river water from the Central Asian headwaters of the Tajikistan Pamirs. *CATENA* **2020**, *193*, 104639. [\[CrossRef\]](#)
- Tian, Y.; Yu, C.Q.; Zha, X.J.; Wu, J.S.; Gao, X.; Feng, C.J.; Luo, K.L. Distribution and Potential Health Risks of Arsenic, Selenium, and Fluorine in Natural Waters in Tibet, China. *Water* **2016**, *8*, 568. [\[CrossRef\]](#)
- Liu, J.T.; Gao, Z.J.; Wang, M.; Li, Y.Z.; Yu, C.; Shi, M.J.; Zhang, H.Y.; Ma, Y.Y. Hydrochemical characteristics and possible controls in the groundwater of the Yarlung Zangbo River Valley, China. *Environ. Earth Sci.* **2019**, *78*, 76. [\[CrossRef\]](#)
- Jiang, L.G.; Yao, Z.J.; Liu, Z.F.; Wang, R.; Wu, S.S. Hydrochemistry and its controlling factors of rivers in the source region of the Yangtze River on the Tibetan Plateau. *J. Geochem. Explor.* **2015**, *155*, 76–83. [\[CrossRef\]](#)
- Zhu, L.P.; Ju, J.T.; Wang, Y.; Xie, M.P.; Wang, J.B.; Peng, P.; Zhen, X.L.; Lin, X. Composition, spatial distribution, and environmental significance of water ions in Pumayum Co catchment, southern Tibet. *J. Geogr. Sci.* **2010**, *20*, 109–120. [\[CrossRef\]](#)

30. Ren, C.B.; Zhang, Q.Q. Groundwater Chemical Characteristics and Controlling Factors in a Region of Northern China with Intensive Human Activity. *Int. J. Environ. Res. Public Health* **2020**, *17*, 9126. [[CrossRef](#)] [[PubMed](#)]
31. Meybeck, M. Global chemical-weathering of surficial rocks estimated from river dissolved loads. *Am. J. Sci.* **1987**, *287*, 401–428. [[CrossRef](#)]
32. Shen, Z.L. *The Basis of Hydrogeochemistry*; Geological Publishing House: Beijing, China, 1993. (In Chinese)
33. Fadili, A.; Najib, S.; Mehdi, K.; Riss, J.; Makan, A.; Guessir, H. Hydrochemical features and mineralization processes in coastal groundwater of Oualidia, Morocco. *J. Afr. Earth Sci.* **2016**, *116*, 233–247. [[CrossRef](#)]
34. Ahmad, T.; Khanna, P.P.; Chakrapani, G.J.; Balakrishnan, S. Geochemical characteristics of water and sediment of the Indus river, Trans-Himalaya, India: Constraints on weathering and erosion. *J. Asian Earth Sci.* **1998**, *16*, 333–346. [[CrossRef](#)]
35. Zhu, B.Q.; Yang, X.P. The ion chemistry of surface and ground waters in the Taklimakan Desert of Tarim Basin, western China. *Chin. Sci. Bull.* **2007**, *52*, 2123–2129. [[CrossRef](#)]
36. Zhang, L.A.; Song, X.F.; Xia, J.; Yuan, R.Q.; Zhang, Y.Y.; Liu, X.; Han, D.M. Major element chemistry of the Huai River basin, China. *Appl. Geochem.* **2011**, *26*, 293–300. [[CrossRef](#)]
37. Ren, X.H.; Gao, Z.J.; An, Y.H.; Liu, J.T.; Wu, X.; He, M.H.; Feng, J.G. Hydrochemical and isotopic characteristics of groundwater in the Jiuquan East Basin, China. *Arab. J. Geosci.* **2020**, *13*, 545. [[CrossRef](#)]
38. Wen, X.H.; Wu, Y.Q.; Wu, J. Hydrochemical characteristics of groundwater in the Zhangye Basin, Northwestern China. *Environ. Geol.* **2008**, *55*, 1713–1724. [[CrossRef](#)]
39. Li, S.Y.; Zhang, Q.F. Geochemistry of the upper Han River basin, China, 1: Spatial distribution of major ion compositions and their controlling factors. *Appl. Geochem.* **2008**, *23*, 3535–3544. [[CrossRef](#)]
40. Sun, R.; Zhang, X.Q.; Wu, Y.H. Major ion chemistry of water and its controlling factors in the Yamzhog Yumco basin, south Tibet. *J. Lake Sci.* **2012**, *24*, 600–608. (In Chinese)
41. Qin, J.; Huh, Y.; Edmond, J.M.; Du, G.; Ran, J. Chemical and physical weathering in the Min Jiang, a headwater tributary of the Yangtze River. *Chem. Geol.* **2007**, *227*, 53–69. [[CrossRef](#)]
42. Li, Y.Z.; Liu, J.T.; Gao, Z.J.; Wang, M.; Yu, L.Q. Major ion chemistry and water quality assessment of groundwater in the Shigaze urban area, Qinghai-Tibetan Plateau, China. *Water Supply* **2020**, *20*, 335–347. [[CrossRef](#)]
43. Yu, J.S.; Zhang, H.B.; Yu, F.J.; Liu, D.P. Characteristics of oxygen isotope composition of atmospheric precipitation in eastern Tibet. *Geochemistry* **1980**, *2*, 113–121. (In Chinese)
44. Craig, H. Isotopic variations in meteoric waters. *Science* **1961**, *133*, 1702–1703. [[CrossRef](#)]
45. Qin, H.H.; Gao, B.; Chen, Y.P.; Sun, Z.X. Spatial Distribution of Hydrogen and Oxygen Isotopes in Lhasa River in Summer and the Implications. *Earth Environ.* **2021**, *49*, 277–284.
46. Dansgaard, W. Stable isotopes in precipitation. *Tellus* **1964**, *16*, 436–468. [[CrossRef](#)]
47. Gu, H.B.; Chi, B.M.; Wang, H.; Zhang, Y.W.; Wang, M.Y. Hydrogen and oxygen stable isotopes and hydrochemical evidence of the transformation relationship between surface water and groundwater in the Liujiang Basin. *Adv. Earth Sci.* **2017**, *32*, 789–799. (In Chinese)